

B-meson rare decays in two-Higgs-doublet models

X.-G. He, T. D. Nguyen, and R. R. Volkas

School of Physics, University of Melbourne, Parkville 3052, Australia

(Received 7 March 1988)

We study $B \rightarrow l^+l^-$, $b \rightarrow sl^+l^-$, and $B \rightarrow Kl^+l^-$ decays in two-Higgs-doublet models. With constraints from $B \rightarrow K^*\gamma$ for the parameters in the model, we find that the branching ratio for $B \rightarrow l^+l^-$ can be two to three orders of magnitude larger than in the standard model, if the Higgs pseudoscalar is very light. The branching ratios for $b \rightarrow sl^+l^-$ and $B \rightarrow Kl^+l^-$ can be an order of magnitude larger than the standard-model predictions.

Recently there have been many studies of the B-meson rare decays $B \rightarrow l^+l^-$, $B \rightarrow Kl^+l^-$, and $b \rightarrow sl^+l^-$ (Ref. 1). These processes are interesting for several reasons. (i) They occur through one-loop interactions and can thus provide useful information about heavy quarks in the loop, consequently testing models beyond the tree level. (ii) Since in these processes the decaying b quark is heavy, long-distance effects are expected to be small compared with short-distance effects and so these processes can be computed reliably. (iii) These decays are not as rare as similar kaon processes. Since the B meson is much heavier than the kaon, the branching ratios can be relatively high in the standard model. The quantity $B(B \rightarrow \tau^+\tau^-)$, for example, which is proportional to the B-meson mass, is in the range $\approx 10^{-9}-10^{-6}$. The branching ratios of the two semileptonic decays we will be considering are proportional to the fifth power of the B-meson mass. Their values in the standard model are in the ranges $B(B \rightarrow Kl^+l^-) \approx 4 \times 10^{-7}-3 \times 10^{-6}$ and $B(b \rightarrow sl^+l^-) \approx 2 \times 10^{-6}-1.5 \times 10^{-5}$ (Ref. 1). These decays are, therefore, experimentally reachable in the near future.

In this paper we carry out calculations for these decays in both versions of two-Higgs-doublet models.² In addition to the standard contributions to these processes, there are contributions due to the extra Higgs particles

that exist in these models. We find that the branching ratio for $B \rightarrow \tau^+\tau^-$ in one of these models can be as high as 10^{-7} , even when the top-quark mass is as low as 40 GeV. This is an increase by 2 orders of magnitude over the standard-model prediction. The branching ratios for $B \rightarrow Kl^+l^-$ and $b \rightarrow sl^+l^-$ can be 1 order of magnitude larger.

We will denote the two Higgs doublets in the model by $\phi_1 = (\phi_1^0, \phi_1^-)$ and $\phi_2 = (\phi_2^0, \phi_2^-)$. After spontaneous symmetry breaking at $\sim M_W$, there exists one charged physical Higgs boson H^+ and one neutral physical pseudoscalar Higgs boson P^0 . These two particles can introduce new contributions to $B \rightarrow l^+l^-$, $B \rightarrow Kl^+l^-$, and $b \rightarrow sl^+l^-$ through "box-" and "penguin-" type diagrams as shown in Fig. 1. [For the moment we do not distinguish between B_d and B_s ; d may be replaced by s in Eqs. (3), (5), (8), and (9) which follow.]

The Lagrangian describing the relevant H^+ interactions is²

$$\mathcal{L}_H = \frac{g}{\sqrt{2}M_W} H^+ \bar{U} V_{KM} (\beta M_u \gamma_- + \delta M_d \gamma_+) D \quad (1)$$

and the P^0 Lagrangian is³

$$\begin{aligned} \mathcal{L}_P = & \frac{g}{2M_W} iP^0 (\beta \bar{U} M_u \gamma_5 U + \delta \bar{D} M_d \gamma_5 D + \delta \bar{l} M_l \gamma_5 l) - \frac{g}{\sqrt{2}M_W} \phi_1^+ \bar{U} V_{KM} (M_u \gamma_- + M_d \gamma_+) D \\ & + \frac{g}{\sqrt{2}} W_\mu^+ \bar{U} \gamma^\mu \gamma_- V_{KM} D + \frac{g}{2} W_\mu^+ (P^0 \gamma^\mu H^- - H^- \gamma^\mu P^0) + \frac{g(M_H^2 - M_P^2)}{2M_W} iP^0 H^+ \phi_1^- + \text{H.c.} , \end{aligned} \quad (2)$$

where for convenience the 't Hooft gauge has been used. ϕ_1^\pm is a fictitious field; M_H and M_P are the masses of H^+ and P^0 , respectively; $U = (u, c, t)$, $D = (d, s, b)$, $l = (e, \mu, \tau)$ and $\nu = (\nu_e, \nu_\mu, \nu_\tau)$; V_{KM} is the Kobayashi-Maskawa matrix. The two different models are distinguished by the choices for β and δ . Model (i) has no ϕ_2 Yukawa terms with U , D , and l and so $\beta = -\delta = \zeta/\eta$, where ζ and η are the vacuum expectation values of ϕ_1^0 and ϕ_2^0 , respectively. Model (ii) has ϕ_1 coupling to U only and ϕ_2 coupling to D

and l and thus, $\beta = 1/\delta = \zeta/\eta$. We first discuss the $B \rightarrow l^+l^-$ decay. The standard-model short-distance contribution to this process is⁴

$$\mathcal{L}_{st} = iM_W^2 \left[\frac{g}{2\sqrt{2}M_W} \right]^4 C(x_i) V_{ib}^* V_{id} M_l f_B \bar{l} \gamma_5 l , \quad (3)$$

where M_l , M_i , and M_W are the lepton, internal quark, and W gauge-boson masses, respectively; $x_i = (M_i/M_W)^2$,

V_{ij} are the Kobayashi-Maskawa matrix elements, and

$$C(x) = \frac{x}{4} + \frac{3x}{4(1-x)} + \frac{3x^2 \ln x}{4(1-x)^2}. \quad (4)$$

We have made use of $\langle 0 | \bar{d} \gamma_5 \gamma^{\mu b} | B \rangle = i f_B P_B^{\mu}$. In the two-Higgs-doublet model, after calculating Fig. 1(a), we obtain the following effective Lagrangian for $B \rightarrow l^+ l^-$:

$$\begin{aligned} \mathcal{L}_{2H} = & \frac{i}{16\pi^2} \left[\frac{g}{2\sqrt{2}M_W} \right]^4 \left[\frac{M_i^3}{M_H^2} f_B \delta^2(\beta^2 M_i^2 - \delta^2 M_b M_d) I(y_i) V_{ib}^* V_{id} \bar{l} \gamma_5 l \right. \\ & \left. + \frac{i}{128\pi^2} (g/M_W)^4 M_i M_i^2 f_B \delta \beta [G_1(x_i, y_i, z) + \beta^2 G_2(y_i)] \frac{M_B^2}{M_P^2 - M_B^2} V_{ib}^* V_{id} \bar{l} l \right], \quad (5) \end{aligned}$$

where M_B is the B -meson mass, $y_i = (M_i/M_H)^2$, $z = (M_H/M_W)^2$, and

$$\begin{aligned} I(y) &= \frac{1}{1-y} + \frac{y \ln y}{(1-y)^2}, \\ G_1(x, y, z) &= \frac{x-2}{2(1-x)} \left[1 + \frac{\ln x}{1-x} \right] + \frac{2}{1-z} \left[\frac{\ln x}{1-x} - \frac{\ln y}{1-y} \right] \\ &+ \frac{1}{2}(1-z) \left[-\frac{z \ln z}{(1-x)(1-z)^2} - \frac{1}{(1-y)(1-z)} - \frac{y \ln y}{(1-x)(1-y)^2} \right. \\ &\left. + \frac{y}{2(1-x)(1-y)} - \frac{1}{2(1-z)(1-x)^2} + \frac{\ln y}{2(1-z)(1-y)^2} \right], \quad (6) \\ G_2(y) &= \frac{y}{2(1-y)} \left[1 + \frac{\ln y}{1-y} \right]. \end{aligned}$$

From these effective Lagrangians, we easily obtain the decay rate $\Gamma_{2H}(B \rightarrow l^+ l^-)$ in the two-Higgs-doublet model,

$$\Gamma_{2H}(B \rightarrow l^+ l^-) = R \Gamma(B \rightarrow l^+ l^-)_{\text{st}}, \quad (7)$$

where, as calculated from Eq. (3),

$$\Gamma(B \rightarrow l^+ l^-)_{\text{st}} = \frac{G_F^4 M_W^4}{32\pi^5} f_B^2 M_B M_i^2 (1 - 4M_i^2/M_B^2)^{1/2} |C(x_i) V_{ib}^* V_{id}|^2 \quad (8)$$

and

$$\begin{aligned} R = & |M_W^2 C(x_i) V_{ib}^* V_{id}|^{-2} \left[\left| \frac{M_i^2 I(y)}{16M_H^2} \delta^2(\beta^2 M_i^2 - \delta^2 M_b M_d) + M_W^2 C(x_i) V_{ib}^* V_{id} \right|^2 \right. \\ & \left. + (1 - 4M_i^2/M_B^2) \frac{M_B^4}{(M_P^2 - M_B^2)^2} \left| \frac{1}{2} \delta \beta M_i^2 (G_1 + \beta G_2) V_{ib}^* V_{id} \right|^2 \right]. \quad (9) \end{aligned}$$

R is a measure of the deviation of the two-Higgs-doublet model from the standard model. From the expression for R we see that the dominating contribution is the second term in Eq. (9) (that is, the one from P^0 -induced effects) if the P^0 is very light. In our later discussion we will take M_P to be zero. A motivation for having a very light P^0 is connected with a possible solution of the strong CP problem.⁵ The first term contains the H^+ -induced contributions, which we see to be suppressed by $(M_i/M_H)^2$. From the way the vacuum expectation values (VEV's) enter into Eq. (9) it is clear that the new contribution from model (ii) is smaller than model (i), if $\zeta/\eta > 1$. We will place emphasis on model (i) for this reason. We notice that the decay width is approximately proportional

to the lepton mass squared. Thus, we deduce that roughly

$$\begin{aligned} \Gamma(B \rightarrow e^+ e^-) : \Gamma(B \rightarrow \mu^+ \mu^-) : \Gamma(B \rightarrow \tau^+ \tau^-) \\ \approx M_e^2 : M_\mu^2 : M_\tau^2. \quad (10) \end{aligned}$$

Also, since $B_d \rightarrow \tau^+ \tau^-$ and $B_s \rightarrow \tau^+ \tau^-$ are dominated by the top-quark internal loop, we have that

$$\frac{B(B_d \rightarrow \tau^+ \tau^-)}{B(B_s \rightarrow \tau^+ \tau^-)} \approx \frac{|V_{dt}|^2}{|V_{st}|^2} \approx \frac{s_{12}^2 s_2^2}{|V_{cb}|^2} < 1, \quad (11)$$

where $s_{1,2} \equiv \sin \theta_{1,2}$ (KM angles). We thus find that $B(B_s \rightarrow \tau^+ \tau^-)$ will be the largest branching ratio among

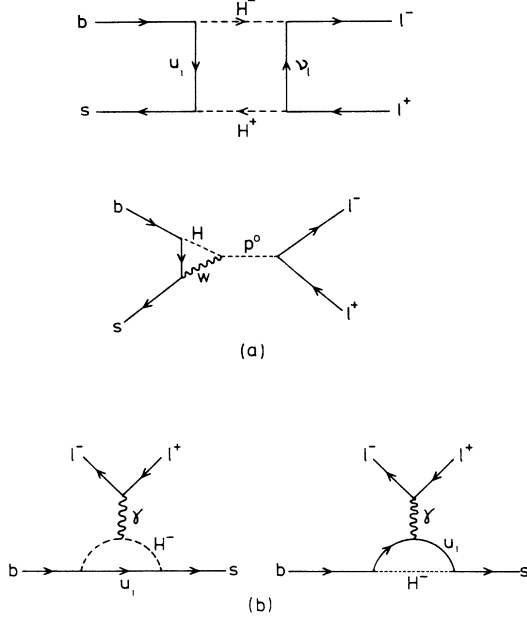


FIG. 1. (a) Generic diagrams for new contributions to $B \rightarrow l^+ l^-$ in the two-Higgs-doublet models. (b) Generic diagrams which together with those in (a) give all new contributions to $b \rightarrow sl^+ l^-$.

the family of $B \rightarrow l^+ l^-$ decays. Note that Eqs. (10) and (11) are approximately valid for both the standard model and the two-Higgs-doublet model. To calculate the branching ratio for $B_s \rightarrow \tau^+ \tau^-$, we normalize the total B_s width to the semileptonic decay width of B_s (Ref. 6),

$$\Gamma(B_s \rightarrow \text{all}) \approx \Gamma(b \rightarrow \text{all}) = \frac{|V_{cb}|^2 G_F^2 m_b^5}{192\pi^3 B_{\text{SL}}} f(m_c/m_b) X_{\text{QCD}}$$

$$\approx 3.3 \frac{|V_{cb}|^2 G_F^2 m_b^5}{192\pi^3}, \quad (12)$$

where B_{SL} is the semileptonic branching fraction of the B meson, and

$$f(x) = 1 - 8x^2 + 8x^6 - x^8 - 24x^4 \ln x, \quad (13)$$

$$X_{\text{QCD}} = 1 - [2\alpha_s(M_b)/3\pi](\pi^2 - \frac{25}{4}).$$

Using $M_B = 5.3$ GeV, $M_b = 4.8$ GeV, and $f_B = 0.1$ GeV we obtain

$$B(B_s \rightarrow \tau^+ \tau^-) = 3.5 \times 10^{-7} |C(x_t)|^2 R. \quad (14)$$

This branching ratio depends on the top-quark mass, the charged-Higgs-boson mass, and the ratio of VEV's. If one assumes that the top quark has the standard branching ratio for the $t \rightarrow be^+ \nu_e$ decay then the top-quark mass is bounded by experimental data from UA1: $M_t > 44$ GeV (Ref. 7). However, it is possible to lower this bound in the two-Higgs-doublet model, provided that the decay mode $t \rightarrow H^+ b$ is kinematically allowed.⁸ In

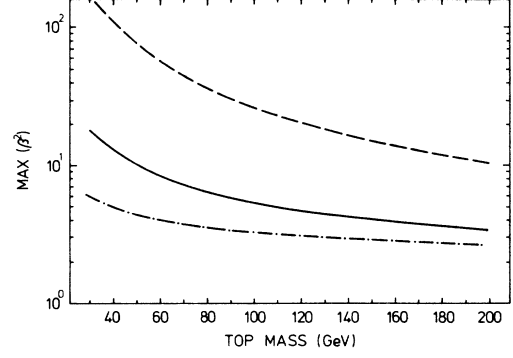


FIG. 2. The upper bound on β^2 as a function of M_t due to $B \rightarrow K^* \gamma$. The dotted-dashed, solid, and dashed lines correspond to $M_H = 30, 100,$ and 500 GeV, respectively.

this case it is possible for the bound to be as low as the KEK TRISTAN value, $M_t > 26$ GeV (Ref. 9). An upper bound for M_t of 200 GeV can be obtained from neutral-current analyses.¹⁰ We will take M_t as a free parameter ranging from 25 to 200 GeV. It is understood that when $M_t < M_H + M_b$ the UA1 lower bound is to be invoked. Constraints on β can be obtained from several sets of experimental data. From $B_S^0 - B_L^0$ mass-difference data it can be shown that $\beta^2 < 4.1 M_H / M_t - 12 M_H / M_t$ provided that $(M_t / M_H)^2 \ll 1$ (Ref. 11). However, this bound depends on other parameters, for example, the bag factor B , which makes this bound unreliable. In Ref. 12, by the use of data from $B \rightarrow K^* \gamma$ and by assuming $B(b \rightarrow s \gamma) \leq 2 \times B(B \rightarrow K^* \gamma)$, it was found that

$$\beta^2 \leq (1.95 - |F_2|) / |H|, \quad (15)$$

where

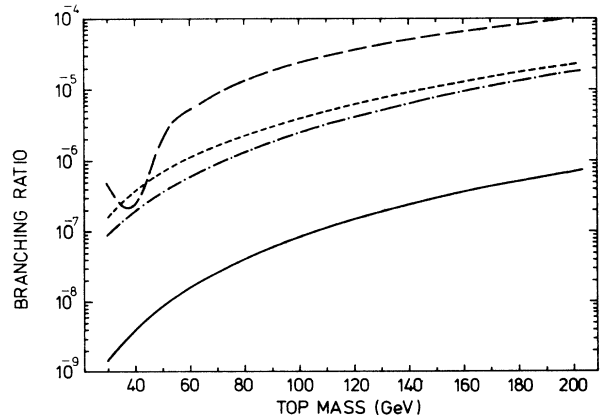


FIG. 3. The solid line is the standard-model prediction for $B(B_s \rightarrow \tau^+ \tau^-)$. The dotted-dashed, short-dashed, and long-dashed lines are the upper bounds on this branching ratio in model (i) for $M_H = 30, 100,$ and 500 GeV, respectively.

$$\begin{aligned}
H(y) &= \beta^2 H_1(y) + \delta \beta H_2(y), \\
H_1(y) &= \frac{y}{12(1-y)^3} \left[Q_i \left[2 + 5y - y^3 + \frac{6y \ln y}{1-y} \right] \right. \\
&\quad \left. - \left[-1 + 5y + 2y^2 + \frac{6y^2 \ln y}{1-y} \right] \right], \\
H_2(y) &= \frac{y}{2(1-y)^3} \left[-Q_i(3-4y+y^2+2 \ln y) + 1 - y^2 \right. \\
&\quad \left. + 2y \ln y \right], \\
F_2(x) &= -Q \left[-\frac{1}{4} + \frac{1-5x-2x^2}{4(1-x)^3} - \frac{3x^2 \ln x}{2(1-x)^4} \right] \\
&\quad + 2T_3 \left[-\frac{3}{4} + \frac{3-9x}{4(1-x)^2} - \frac{3x^2 \ln x}{2(1-x)^3} \right],
\end{aligned} \tag{16}$$

where Q_i is the electric charge of the internal fermion, and Q and T_3 are the electric charge and the weak charge of the external quark. This bound is stronger than the one from B_S^0 - B_L^0 mass difference. Constraints on β can also be obtained from $K_L \rightarrow \mu^+ \mu^-$ by doing an analysis similar to $B \rightarrow l^+ l^-$. However, because of long-distance effects we can only obtain an upper bound on β which is slightly weaker than bounds obtained from $B \rightarrow K^* \gamma$. Consequently in our later discussions we will use constraints on β from $B \rightarrow K^* \gamma$. The bounds are plotted as a function of M_t in Fig. 2. This plot relates to model (i)

$$E(y) = \frac{y\beta^2}{36(1-y)^3} \left[Q_i \left[-16y + 29y^2 - 7y^3 - \frac{6y(2-3y) \ln y}{1-y} \right] + \left[-2 + 7y - 11y^2 - \frac{6y^3 \ln y}{1-y} \right] \right]. \tag{18}$$

Diagrams in Fig. 1(a) also contribute to this process, but is suppressed by a factor $(M_t/M_W)^2$ compared with the contribution from Fig. 1(b). We will neglect this term in our subsequent discussion. We also neglect the small contribution due to Z^0 exchange, to obtain¹

$$\begin{aligned}
\Gamma(b \rightarrow sl^+ l^-) &= \frac{G_F^2 M_b^5}{192\pi^3} \left[\frac{g^2}{16\pi^2} \right]^2 T, \\
T &= |\lambda_i A_i| + |\lambda_i B_i| + 4s_W^2 \lambda_i (A_i + B_i) \lambda_j F'_{2j} + 16s_W^4 [\ln(M_b/2M_t) - \frac{2}{3}] |\lambda_i F'_{2i}|^2,
\end{aligned} \tag{19}$$

where $s_W \equiv \sin \theta_W$ (θ_W = Weinberg angle) and

$$\begin{aligned}
B_i &= -s_W^2 [F'_{1i} + 2C^z(x_i)], \quad A_i = C(x_i) + B_i, \\
F'_{2i} &= F_2(x_i) - H(y_i), \quad F'_{1i} = F_1(x_i) + E(y_i), \\
\lambda_i &= V_{is}^* V_{ib}.
\end{aligned} \tag{20}$$

The form factors C and C^z can be found in Ref. 4. Setting E and H to zero restores the standard-model result. To obtain the decay amplitude for $B \rightarrow Kl^+ l^-$ we use

$$A(B \rightarrow Kl^+ l^-) = \langle Kl^+ l^- | \mathcal{L} | B \rangle. \tag{21}$$

We thus have¹³

$$\begin{aligned}
\Gamma(B \rightarrow Kl^+ l^-) &= \frac{G_F^2 M_b^5}{192\pi^3} \left[\frac{g^2}{16\pi^2} \right]^2 \frac{f_+(0)}{8} \\
&\quad \times [|\lambda_i a_i|^2 + |\lambda_i C(x_i)|^2], \\
a_i &= C(x_i) - 2s_W^2 [F'_{1i} + 2C^z(x_i)] - 2(M_b/M_B)^2 s_W^2 F'_{2i}.
\end{aligned} \tag{22}$$

since not only is the new contribution to the decay larger than in model (ii), but also the above bound is more stringent due to a larger form factor H . Throughout the paper we plot all quantities of interest as functions of M_t with some representative values of M_H : 30, 100, and 500 GeV.

Using the bounds from Fig. 2, the upper bounds on $B(B_s \rightarrow \tau^+ \tau^-)$ in model (i) and the standard-model prediction are plotted in Fig. 3. The bounds, in general, are increasing functions of M_H and M_t . Note also that in the two-Higgs-doublet model $B(B_s \rightarrow \tau^+ \tau^-)$ can be as large as 10^{-4} , and values of the order of 10^{-7} are possible even for small M_t (≈ 30 GeV), which is an increase of 2 orders of magnitude over the standard-model result. Thus, this decay may provide a good test of this model.

We now discuss the decays $b \rightarrow sl^+ l^-$ and $B \rightarrow Kl^+ l^-$. The effective photon-exchange Lagrangian in two-Higgs-doublet models, from Fig. 1(b), is¹²

$$\begin{aligned}
\mathcal{L} &= \frac{eg^2}{32\pi^2 M_W^2} \sum_i V_{ia} V_{ib}^* (\bar{B} V^{\mu} A) A_{\mu}, \\
V^{\mu} &= iq_{\nu} \sigma^{\mu\nu} (M_a \gamma_+ + M_b \gamma_-) (F_2 - H) \\
&\quad + (q^2 \gamma^{\mu} - q^{\mu} \not{q}) (F_1 + \beta^2 y_i G) \gamma_-.
\end{aligned} \tag{17}$$

F_1 and F_2 are contributions due to the W boson in the standard model and are given in Ref. 4. H and G are contributions¹² due to H^+ . H is given in Eq. (16) and $E(y) = \beta^2 y G(y)$ is given by

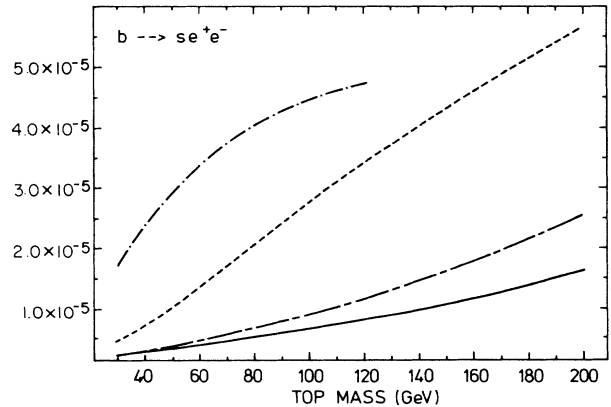


FIG. 4. Variation of $B(b \rightarrow se^+ e^-)$ with respect to M_t and M_H for a fixed value of $\beta^2 = 3$. The short-dashed-long-dashed, dashed, and dotted-dashed lines correspond to $M_H = 500, 100,$ and 30 GeV in model (i). The 30 GeV line is cut off at $M_t \approx 120$ GeV because of the bound from $B \rightarrow K^* \gamma$ (see Fig. 2). The solid line is the standard-model prediction.

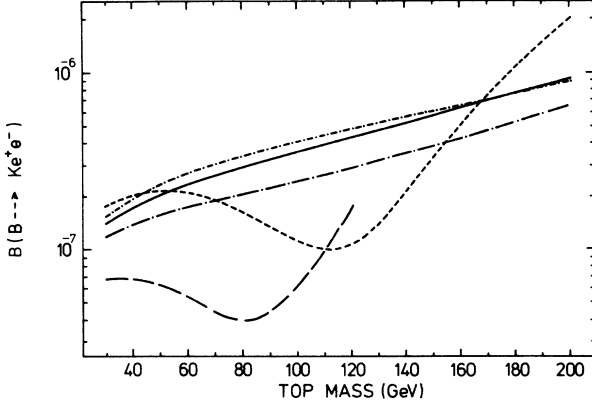


FIG. 5. The solid line is the standard model $B(B \rightarrow Ke^+e^-)$. The long-dashed and dotted-long-dashed lines are predictions in model (i) for $M_H=30$ and 100 GeV, respectively. The short-dashed and dotted-short-dashed lines are predictions in model (ii) for $M_H=30$ and 100 GeV, respectively. $\beta^2=3$ for all the two-Higgs-doublet model lines.

To obtain Eq. (22) we have used

$$\langle K | \bar{s}\gamma^\mu b | B \rangle = f_+(q^2)(P_B + P_K)_\mu + f_-(q^2)(P_B - P_K)_\mu, \quad (23)$$

$$\langle K | \bar{s}i\gamma_\nu\sigma^{\mu\nu}b | B \rangle = h(q^2)(P_{B\mu}P_{K\nu} - P_{B\nu}P_{K\mu})q^\nu.$$

Assuming B^* vector-meson dominance, nonrelativistic bound-state quark dynamics, and the spectator model, we have¹⁴

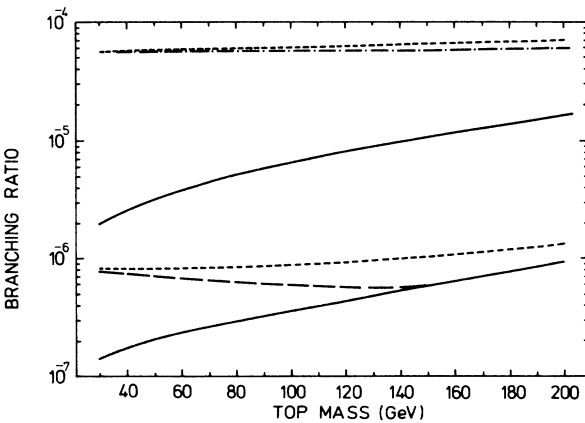


FIG. 6. The upper and lower solid lines are the standard-model predictions for $B(b \rightarrow se^+e^-)$ and $B(B \rightarrow Ke^+e^-)$, respectively. The upper short-dashed line is the upper bound on this branching ratio for both $M_H=100$ and 500 GeV. The dotted-dashed line next to that is the upper bound for $M_H=30$ GeV. The two lower short-dashed and long-dashed lines are upper bounds on $B(B \rightarrow Ke^+e^-)$ for $M_H=30$ and 500 GeV, respectively.

$$f_+(q^2) = \left[\frac{M_{B^*}^2}{M_{B^*}^2 - q^2} \right] f_+(0),$$

$$h(q^2) = 2(M_s + M_b)f_+(q^2)/M_{B^*}^2, \quad (24)$$

$$f_+(0) = \frac{f_B M_B}{f_K M_{B^*}}.$$

Normalizing the total width of the B meson to the semi-leptonic decay width, we obtain the branching ratios

$$B(b \rightarrow sl^+l^-) = 1.93 \times 10^{-6} T, \quad (25)$$

where T is given in Eqs. (19) and (20) and

$$B(B \rightarrow Kl^+l^-) = 2.4 \times 10^{-7} [|a|^2 + |C(x)|^2] f_+^2(0). \quad (26)$$

The results are plotted in Figs. 4–6.

For $b \rightarrow sl^+l^-$, the situation is similar to that of $B_s \rightarrow \tau^+\tau^-$ in that the enhancement in model (i) is much larger than that in model (ii), so we again focus on model (i). Figure 4 shows the variation of $B(b \rightarrow se^+e^-)$ with M_H and M_t for a fixed value $\beta^2=3$. The curve for $M_H=30$ GeV is cut at $M_t \approx 120$ GeV due to the bound in Fig. 2.

For $B \rightarrow Kl^+l^-$, however, there is a partial cancellation between the H^+ contribution and the W contribution in model (i), whereas in model (ii) they add. This effect is exactly opposite to that in $b \rightarrow sl^+l^-$. This occurs because the H form factor in model (i) always has the opposite sign to that in model (ii). Note also the sign difference of the F_2 terms in Eqs. (19) and (22). To illustrate this we show the deviations from $B(B \rightarrow Ke^+e^-)_{st}$ in both models in Fig. 5, for a common value $\beta^2=3$. Note the difference between predictions for small M_H (≈ 30 GeV) and relatively large M_H (> 100 GeV). The explanation lies in the fact that for relatively large M_H the form factor E is negligible compared to H , while for small M_H it is not. The curve for $M_H=30$ GeV in model (i) is cut at $M_t=120$ GeV due to the bound in Fig. 2. Finally, Fig. 6 shows the upper bounds for $B(b \rightarrow se^+e^-)$ and $B(B \rightarrow Ke^+e^-)$ in model (i). The upper bound on $B(b \rightarrow se^+e^-)$ is essentially independent of M_H , because the numerical factor $16s_W^4 [\ln(M_b/2M_e) - \frac{2}{3}]$ appearing in the term $|F_2|^2$ in Eq. (19) is so large that the maximum branching ratio is well approximated by taking the maximum value of F_2 . From the experimental bound on $B \rightarrow K^*\gamma$ we have $F_2 \leq 1.95$. For $B \rightarrow Ke^+e^-$ this also holds for relatively large M_H (> 100 GeV). However, for small M_H (≈ 30 GeV) the form factor E actually dominates, because its numerical

factor is about twice as large as that of F_2 and also because $E > H$ for small M_H [see Eq. (22)].

In conclusion, then, we have demonstrated that present bounds on the ratio of VEV's β in the two-Higgs-doublet model permit a substantial increase in the branching ratios of rare B -meson decays compared with standard-model values. We await with interest the new generation

of experiments which may discover evidence for an extended Higgs sector.

X.-G.H. would like to thank Professor B. H. J. McKellar for valuable discussions. We would like to acknowledge support by the Australian Research Grants Committee.

-
- ¹N. Deshpande, G. Eilam, A. Soni, and G. Kane, *Phys. Rev. Lett.* **57**, 1106 (1986); G. Eilam, J. Hewett, and T. Rizzo, *Phys. Rev. D* **34**, 2773 (1986); W.-S. Hou, R. S. Wiley, and A. Soni, *Phys. Rev. Lett.* **58**, 1608 (1987).
²H. Haber, G. Kane, and T. Sterling, *Nucl. Phys.* **B161**, 493 (1979); L. Abbott, P. Sikivie, and M. Wise, *Phys. Rev. D* **21**, 1393 (1980).
³L. Hall and M. Wise, *Nucl. Phys.* **B187**, 397 (1981).
⁴T. Inami and C. S. Lim, *Prog. Theor. Phys.* **65**, 297 (1981); **65**, 1772(E), (1981).
⁵R. Peccei and H. Quinn, *Phys. Rev. Lett.* **38**, 1440 (1977); S. Weinberg, *ibid.* **40**, 223 (1978); F. Wilczek, *ibid.* **40**, 279 (1978).
⁶See, for example, J. R. Cudell, F. Halzen, X.-G. He, and S. Pakvasa, *Phys. Lett. B* **196**, 227 (1987).

- ⁷UA1 Collaboration, CERN Report No. CERN EP/87-190 (unpublished).
⁸S. L. Glashow and E. E. Jenkins, *Phys. Lett. B* **196**, 233 (1987); V. Barger and R. J. N. Phillips, *Phys. Lett. B* **201**, 553 (1988).
⁹F. Takasaki, report to Hamburg Conference, 1987 (unpublished).
¹⁰U. Amaldi *et al.*, *Phys. Rev. D* **36**, 1385 (1987); G. Costa *et al.*, *Nucl. Phys.* **B297**, 244 (1988).
¹¹G. G. Athanasiu *et al.*, *Phys. Rev. D* **32**, 3010 (1985).
¹²T. D. Nguyen and G. C. Joshi, *Phys. Rev. D* **37**, 3220 (1988).
¹³K. Babu, X.-G. He, X.-Q. Li, and S. Pakvasa, *Phys. Lett. B* **205**, 540 (1988).
¹⁴M. Suzuki, Berkeley Report No. LBL 23954, 1987 (unpublished).